

VI RUSSIAN CONFERENCE
ON CATALYTIC REACTION MECHANISMS
(Moscow, October 1–5, 2002)

The Study of the Nature of Adsorbed Species
to Build a Bridge between Surface Science and Catalysis:
Problems of Pressure and Material Gap

V. I. Bukhtiyorov

Boreskov Institute of Catalysis, Siberian Division, Russian Academy of Sciences, Novosibirsk, 630090 Russia

Received December 17, 2002

Abstract—This review substantiates the molecular approach to the study of the catalytic action of various systems, which consists in the comparative study of the nature and reactivity of adsorbed species and considering the problems of pressure and material gaps. The pressure gap problem can be solved by a continuous increase in the pressure of the reaction mixture, including carrying out *in situ* studies. The solution to the problem of material gap is possible when one passes from bulk to dispersed samples, which model real supported catalysts. As the last step that can build a bridge between surface science and catalysis, the study of nanoparticle reactivity toward the reactants of a catalytic reaction with varying sizes of nanoparticles is proposed. The scope of such an approach is demonstrated by the study of silver catalysts of ethylene epoxidation. It was found that the catalytic action of silver in the process of ethylene oxide synthesis is determined by the possibility of formation of electrophilic adsorbed atomic oxygen. Its formation is more efficient under the action of reaction mixtures at high pressures and on the surfaces of silver species with sizes smaller than 50 nm. It is shown that the reaction center should also contain the nucleophilic form of O_{ads} , which itself is only active in the complete oxidation of ethylene but creates the Ag^{1+} sites for ethylene adsorption. The disappearance of O_{nucl} with a decrease in the size of silver particles below 50 nm leads to a drastic decrease in the rate of ethylene epoxidation. The reaction mechanism made it possible to propose systems with an abnormally high value of selectivity to ethylene oxide (>90%).

INTRODUCTION

Most papers devoted to mechanistic studies of heterogeneous catalytic reactions by surface-sensitive physical methods are motivated by the desire of researchers to use their findings to purposefully improve the catalysts. In recent years this approach (development of new catalysts on the basis of mechanistic data) becomes more and more popular, and the number of papers demonstrating success in using such an approach grows from one year to another (see, for instance, [1–4]). This line of research currently dominates surface science.

The mechanism of chemical reaction is a set of elementary steps resulting in the transformation of reactants into the reaction products. In the case of heterogeneous catalytic reactions, which will be considered in this review, an important place in such a sequence of steps is filled by the steps of reactant adsorption on the catalyst surfaces. Indeed, these steps are responsible for reactant activation, the formation of adsorption states with unusual properties, the elimination of symmetry constraints, etc. In the end, all these factors favor the occurrence of a chemical reaction in the presence of a catalyst. Therefore, from the 1970s, when commercially available spectrometers for surface studies (LEED, Auger, and XPS) appeared, researchers started to give considerable attention to the study of adsorption

processes. There are hundreds of publications on this subject.

However, it should be noted that the conditions for most such experiments are very far from real conditions of catalytic reactions. Indeed, pressures at which most physical methods of surface studies are applicable ($P < 10^{-4}$ Pa) are several orders of magnitude lower than those used in catalytic reactions ($P > 10^5$ Pa). This forms the basis for the so-called pressure gap problem. Another difference between model studies carried out using physical methods and real catalytic processes is the use of single crystalline metal surfaces, whereas catalysts are small metal particles supported on the surface of an inert support matrix. The metal particles are so small (often smaller than 3–5 nm) that one should take into consideration the difference between the properties of the dispersed metal and the properties of the bulk sample. Thus, a material gap problem arises.

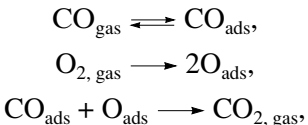
From the 1980s, researchers have devoted more attention to solving the above problems in order to efficiently use the results of model studies to explain or even predict the specific features of the catalytic action of certain systems. To solve the problem of pressure gap, high-vacuum chambers of spectrometers were equipped with various high-pressure cells where the samples under study interacted with the reaction mixture and with systems for the fast loading of samples

into the spectral zone for further analysis of changes. For instance, in [5, 6], the composition of adlayers on silver single crystals were analyzed by such physical methods as Auger spectroscopy, XPS, TPD, and LEED, even 15–20 s after sample treatment with the mixtures of ethylene and oxygen. In the course of treatment at high pressures, the authors were able to measure the activities of silver samples in ethylene oxidation using mass spectrometry. The lack of contact of the sample with an ambient atmosphere when it was transferred from the reaction zone into the zone for analysis allowed the authors to hope that changes that occurred under the action of the reaction medium can be monitored by physical methods. However, the main drawback of postreaction analysis was preserved: the evacuation of the reaction mixture results in the disappearance of weakly adsorbed species because of their desorption, whereas these species might determine the activities of the catalyst samples under reaction conditions.

This drawback can be eliminated if another approach to solving the pressure gap problem is used. It consists in the application or development of physical methods that are workable at pressures used in catalysis (of the order of $\geq 10^2$ Pa or higher). This makes it possible to obtain quantitative correlations between the catalytic characteristics of the sample and the compositions of adlayers on its surface. Among such methods that allow *in situ* studies, we should mention X-ray photoelectron spectroscopy (XPS), X-ray absorption near-edge structure (XANES), polarization modulation infrared absorption spectroscopy (PM IRAS), and sum frequency generation (SFG). Examples of the use of these physical methods in the studies of adsorbed species formed at high pressures ($P > 10^2$ Pa) can be found in [7–12].

Development of methods for reproducible application of model supported catalysts for further studies of their electron properties and the structure of the surface of supported metal particles depending on their size is the first step in solving the problem of material gap [13, 14]. The first attempts to study adsorption on dispersed metal particles were also made in [15–17]. It was shown that the replacement (physical modeling) of supported catalysts by model samples in which dispersed particles are supported on the surface of planar support makes it possible to avoid difficulties in carrying out adsorption experiments: difficulties in the preparation of atomically pure surfaces (high-temperature heating, which is often used to clean the surfaces of bulk samples, may lead to particle sintering), the overlap of spectral characteristics of a support and an adsorbate, and a low specific concentration of adsorption sites on supported catalysts compared to bulk samples. This makes it possible to obtain new experimental data on the nature of adsorbates. At the same time such model systems cannot be used to measure the catalytic properties.

In our opinion, in order to build a bridge between surface science and catalysis, it is necessary to study in detail the reactivity of supported particles toward the reactants of the catalytic reaction with the sizes in the same range as in the catalysts used in the reaction under consideration. Let us demonstrate this using the CO oxidation reaction catalyzed by platinum-group metals as an example. The study of the effect of the size of palladium particles supported in $\alpha\text{-Al}_2\text{O}_3$ in CO oxidation showed [18] that a decrease in the average size below 5 nm leads to a threefold increase in the reaction rate. This result was explained by the standard Langmuir–Hinshelwood mechanism:



determined earlier in the studies of this reaction over single crystal surfaces [19, 20], and by the weakening of the CO–Pd bond in the case of small clusters. This conclusion was based on the results of the comparative TPD study of CO adsorption on the Pd(111) surface and on the surface of dispersed palladium [20, 21]. It was shown that, in the TPD spectrum of CO for palladium particles with a size of 2.5 nm, an additional state with a lower temperature of desorption is observed compared to the spectrum for the single crystalline surface, whereas the spectrum for large particles ($d = 27$ nm) is identical to the spectrum of single crystals. Weakly bound CO molecules are responsible for the high rate of the reaction $\text{CO} + \text{O}_2$ in the case of small palladium clusters.

A radically different behavior of TPD spectra of CO was found for platinum particles supported on aluminum oxide [22] or mica [23]: the weakly bound state registered in the case of single crystals or large particles of supported platinum almost disappears when the size of platinum particles decreases below 3 nm. This result is in complete agreement with more than sevenfold decrease in the rate of CO oxidation on small platinum clusters [24].

The comparative TPD study of CO adsorption on supported platinum and rhodium [25] showed that the relative formation of weakly and strongly bond CO_{ads} species is practically independent of the average size of dispersed rhodium particles. This is a probable reason for the absence of structural sensitivity of the $\text{CO} + \text{O}_2$ reaction on rhodium in contrast to the same reaction on palladium and platinum [26].

Success in explaining the difference in the behavior of platinum-group metals in the reaction of CO oxidation (the positive “size” effect for palladium, the negative effect for platinum, and the absence of the effect on rhodium) stimulated the use of such an approach in studies of other catalytic systems [27, 28]. However, we should confess that the more complicated the catalytic reaction, the less data there are available based on mechanistic studies using physical methods. In our lab-

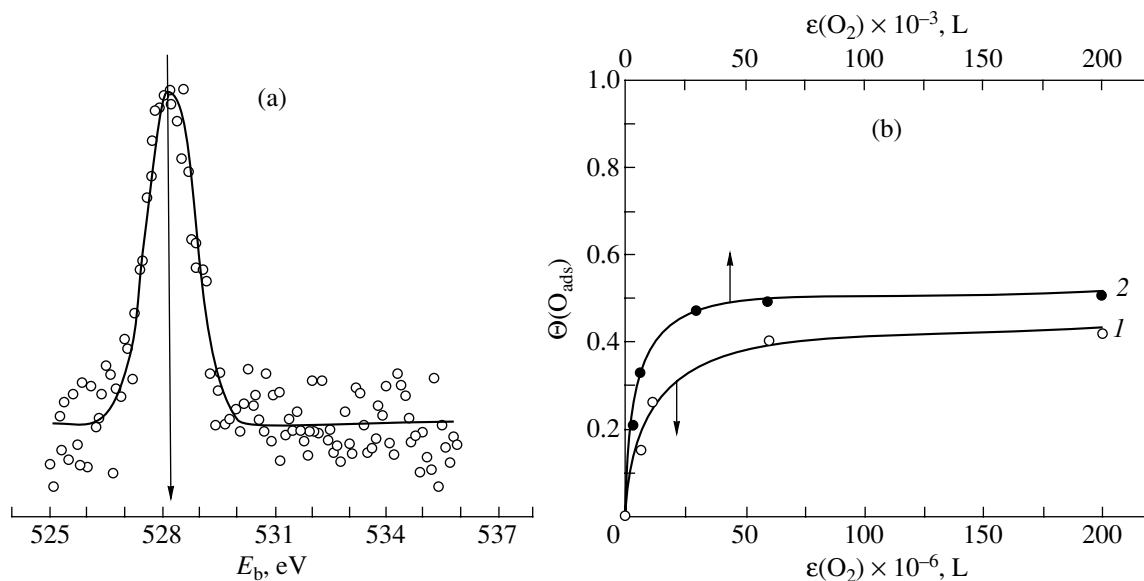


Fig. 1. (a) XPS spectrum O1s recorded after oxygen adsorption on the Ag(111) surface for 5 min at $T = 420$ K and $P_{O_2} = 10$ Pa; (b) dependence of the silver surface coverage with adsorbed oxygen ($\Theta(O_{ads})$) on O_2 exposure ($\epsilon(O_2)$) measured for (1) Ag(111) and (2) Ag(110).

oratory, this approach is used to study ethylene epoxidation on silver, the partial oxidation of methanol to formaldehyde on copper, the effect of cesium promoters on silver catalysts, and the effect of SO_2 on platinum catalysts for CO oxidation and the selective oxidation of hydrocarbons by a mixture of oxygen and hydrogen. This paper is devoted to the first line of our research listed here, namely, the mechanistic study of the action of silver catalysts for ethylene epoxidation. Despite numerous papers devoted to the study of this system (see, for instance, [5–6, 29–32]) motivated by the uniqueness of silver as a catalyst for ethylene epoxidation, the mechanism of this reaction is debated. The main question concerns the nature of the adsorbed oxygen that epoxidizes ethylene to ethylene oxide.

RESULTS AND DISCUSSION

The adsorption of O_2 on clean single crystal Ag(111) and Ag(110) surfaces at $T = 470$ K leads to the formation of adsorbed oxygen characterized by the XPS signal O1s with the binding energy $E_b = 528.4$ eV (Fig. 1a) and the desorption temperature ~ 570 K. These characteristics were observed many times in other studies and suggest the formation of surface oxide [5–6, 31–33]. Furthermore, the results of experiments on the temperature-programmed reaction of this adsorbed state with adsorbed ethylene are in complete agreement with literature data [5–6, 31]: only the products of complete oxidation are registered in TPR spectra. Therefore, following terminology proposed in [29], henceforth we will refer to this form of O_{ads} as nucleophilic. The only difference in the behavior of Ag(111) and

Ag(110) surfaces is the value of O_2 exposure required for surface saturation with nucleophilic oxygen (Fig. 1b): 5×10^4 L (1 L = 1 s $\times 10^{-6}$ Torr) in the case of Ag(110) and 5×10^7 L in the case of Ag(111). A further increase in P_{O_2} does not lead to the formation of additional states of adsorbed oxygen. As a consequence, the activity in ethylene epoxidation is not observed. This result supports the well-known conclusion of many authors that clean silver is inactive in ethylene epoxidation and it should be activated by the reaction mixtures at high pressures [29, 30].

1. Pressure Gap Problem

The interaction of the reaction mixture with the surface of bulk silver (Ag(111), Ag(110), or polycrystalline foil) at pressures of the order of 10^2 Pa leads to the appearance of the new XPS signal O1s with a binding energy of 530.5 eV (Fig. 2a). The identification of this signal requires additional experiments, because similar values of E_b in the literature were assigned to surface hydroxy groups [34, 35] or carbonates [6, 36], which are readily formed at high exposures due to the interaction of adsorbed oxygen with background H_2O and CO_2 . Analysis of the spectrum of the valence zone (Fig. 2b) recorded after similar treatment helps to solve this problem. It is well known that OH_{ads} and $CO_{3, ads}$ species show typical signals below the Ag4d zone. Because in our case we did not observe any peaks in this spectral (Fig. 2b), we assume that the treatment of silver by the reaction mixture leads to the formation of the new form of adsorbed oxygen.

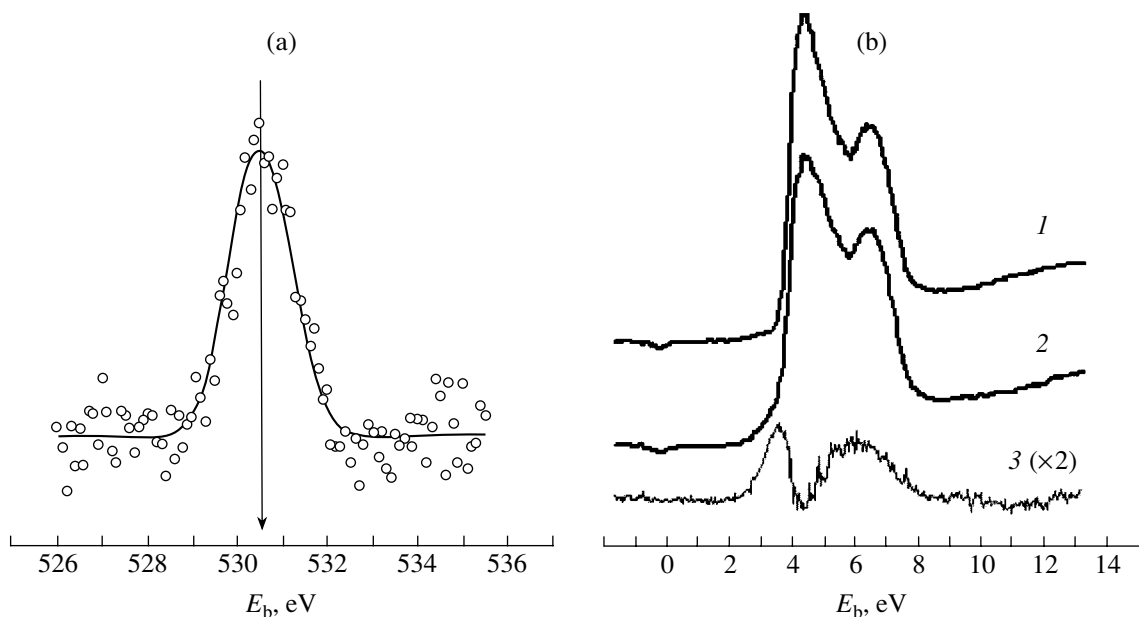


Fig. 2. (a) XPS spectrum O_{1s} and (b) the spectra of the valence zone: (1) clean surface and (2) after treatment of the surface of silver foil with the reaction mixture 2% C₂H₄ + O₂ for 30 min at T = 420 K and a total pressure of 10² Pa; (3) the difference spectrum 2–1.

The results of testing the reactivity of this oxygen species toward ethylene are shown in Fig. 3. ¹⁸O₂ was used to form nucleophilic oxygen, whereas the second adsorbed oxygen species was studied using a mixture of ¹⁶O₂ with ethylene (Fig. 3a). Ethylene adsorption on an isotopically labeled layer of adsorbed oxygen and further heating of the silver with simultaneous TPR spectrum recording proves that oxygen species formed under the action of the reaction medium participates in ethylene epoxidation. Indeed, we observed only the signal with *m/z* = 29 (C₂H₄¹⁶O) in the TPR spectra of ethylene oxide, whereas the signal with *m/z* = 31 (C₂H₄¹⁸O) is completely absent (Fig. 3b). In contrast, nucleophilic oxygen provides the formation of C¹⁸O₂ with *m/z* = 48. Taking into account the activity of the second state of adsorbed oxygen in the formation of ethylene oxide, we will refer to it as “electrophilic”, as in [29].

A considerable increase (2.1 eV) in the value of the binding energy in the case of electrophilic oxygen compared to nucleophilic oxygen stimulated discussion in the literature, which continues to this day. Some authors insist on the fact that electrophilic oxygen, like nucleophilic, is atomic [29–31]. Others suggest that this is a molecular or even ozone-like species [5, 6, 32]. We chose XANES to resolve the issue. XANES experiments were carried out in collaboration with the Department of Inorganic Chemistry at the Fritz Haber Institute (Berlin, Germany) using the Berlin source of synchrotron irradiation BESSY-I. X-ray absorption occurs due to electron transitions from internal levels to vacant valence orbitals [37]. The mechanism of such interaction of X rays with the substance can be explained using the example of an oxygen molecule (Fig. 4a). Following the selection rule (transitions are

allowed only if the orbital quantum number changes by unity), only electron transitions from the 1s level to vacant orbitals that have the 2p character or antibonding 1π_g or 3σ_u character are active. Therefore, the XANES spectra of molecular oxygen have a typical π*/σ* structure, which is preserved even in the chemisorbed state despite shifts (Fig. 4b). It is the sensitivity of XANES to the structure of oxygen molecular orbitals that explains our choice of XANES for the study of electrophilic oxygen.

Figure 5 shows the O K-edge spectrum from electrophilic oxygen recorded after the treatment of polycrystalline silver foil with a mixture of ethylene and oxygen for 30 min at *P* = 2 × 10² Pa and *T* = 470 K, together with the spectra of peroxy O_{2,ads} chemisorbed on the Ag(110) surface (for comparison) [38]. The individual formation of electrophilic oxygen on the surface of the same silver foil was controlled by XPS. It can be seen that the spectral region of electrophilic oxygen that is characteristic of the molecular orbital (530–535 eV) does not contain any visible signals. This allows us to conclude that this state of oxygen is atomic. The results of detailed analysis of the nature of the nucleophilic and electrophilic states of atomically adsorbed oxygen carried out on the basis of data obtained by XPS, UV spectroscopy, XANES, and Auger spectroscopy are presented in [39].

Thus, silver activation in ethylene epoxidation (by the treatment of the clean surface with the reaction mixture at high pressures, a solution to the pressure gap problem) is due to the formation of an additional form of atomic oxygen (O_{elec}), which differs in the value *E_b(O_{1s})* from the form that is seen in the case of O₂ on

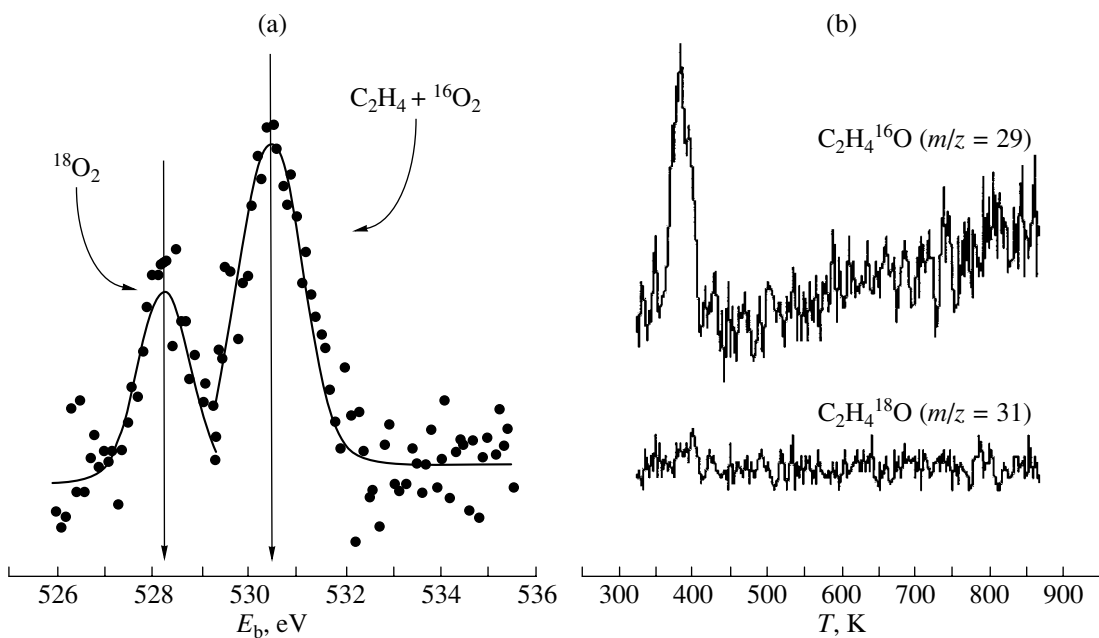


Fig. 3. (a) XPS spectrum O1s and (b) TPR spectra of ethylene oxide recorded after the treatment of the silver foil surface with the reaction mixture 5% $\text{C}_2\text{H}_4 + ^{16}\text{O}_2$ at $P = 10^2$ Pa and $T = 470$ K and further $^{18}\text{O}_2$ adsorption at $P = 10^{-2}$ Pa and $T = 420$ K.

the clean surface (O_{nucl}). However, we admit that experimental conditions for data presented in Figs. 2, 3, and 5 refer to the postreaction period and these conditions may not allow the registration of adsorbed species that exist only under reaction conditions and probably disappear upon evacuation of the gas phase before photoelectron spectrum recording. This problem can be solved by carrying out experiments where analysis of the composition of adlayers is carried out in the course of a catalytic reaction (e.g., by the XANES method in the regime of complete photocurrent measurement used by us). Obviously, the vacuum system of a spectrometer should allow one to maintain a constant flow of reaction gases through the measurement cell. In our case, this was achieved by using the turbomolecular pump and two mass-flow controllers (for oxygen and methanol) [9]. The schematic of the high-pressure chamber of the XANES spectrometer is shown in Fig. 6a. In addition to the sample under study, it contains two detectors, which makes it possible to measure the absorbance of X-rays in the gas phase. Further subtraction of this signal from the overall signal gives the sample signal (Fig. 6b).

Indeed, it can be seen that gaseous O_2 contributes greatly to the O K -edge sample spectrum. Only after its subtraction is it possible to obtain the spectrum of the silver surface. It appears that the difference spectrum is rather close to the spectrum of electrophilic oxygen. This makes it possible to conclude that the electrophilic form of adsorbed oxygen is the main species on the silver surface under reaction conditions.

At the same time, this conclusion needs one comment: it only applies to the samples of bulk silver. On the other hand, commercial catalysts are silver particles supported in the surface of α -alumina, and this may be one of the reasons for the material gap problem.

2. Material Gap Problem

Switching from bulk samples to dispersed particles may cause changes in electron, structural, and adsorption characteristics of a metal, and this should be taken into account when studying its catalytic properties and how they change depending on the size of particles. To study the size effects on supported silver catalysts, we prepared special model samples, which are silver samples on a graphite surface. The replacement of the oxide support (Al_2O_3) by carbon makes it possible to avoid the effect of recharging, which in the case of nonconducting samples makes the study of electron properties of supported metal samples difficult. This also allows one to remove the masking effect of the O1s signal from the support and use the XPS method to study O_2 adsorption on the surface of supported silver [16, 40]. Of course, silver deposition and further oxygen adsorption on the surface of model Ag/C samples was carried out without contact of samples with an oxygen atmosphere. Only the sizes of deposited silver particles were tested by the scanning tunneling microscopy (STM) method in air after sample discharging from the spectrometer. Figure 7 shows STM images of the graphite surface before and after silver deposition for one of the coverages, which was expressed in terms of the relative intensities of XPS signals of silver and carbon: $I_{\text{Ag}3d}/I_{\text{Cl}1s} = 13.1$.

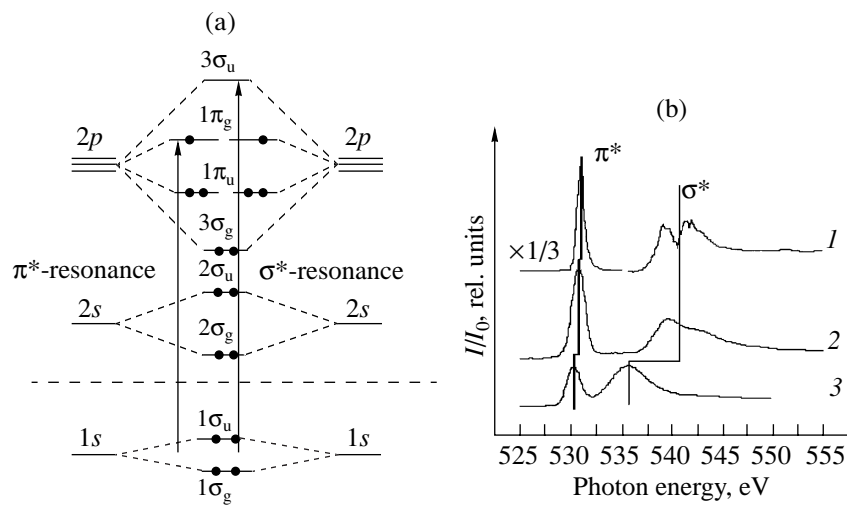


Fig. 4. (a) Scheme of electron transitions in the oxygen molecule upon consuming an X-ray quantum; (b) experimental XANES O K-edge spectrum of various O_2 molecule states [37]: (1) O_2 , gas; (2) O_2 , physisorbed/Pt(111); and (3) O_2 , chemisorbed/Pt(111).

It can be seen that, in contrast to a clean graphite surface, which is rather smooth, the surface is characterized by increased roughness due to the formation of three-dimensional silver particles upon deposition. Their average size is 20–30 nm. STM measurements were carried out only for certain silver coverages, whereas the XPS estimates of the amount of deposited silver were made over the whole range of coverages.

Figure 8a shows $Ag3d_{5/2}$ spectra for several coverages recorded after silver deposition. It can be seen that the lowest of silver coverages is characterized by the $Ag3d_{5/2}$ band with $E_b = 368.9$ eV, whereas an increase in the coverage or, more exactly, an increase in the size of silver particles leads to a constant shift in the spectrum toward lower binding energies. Such a behavior (an increase in the value of E_b with a decrease in the size of supported particles below 3–5 nm) has been observed earlier for many metals including silver [41, 42] and it was explained by either metal–dielectric transition (a change in the initial state) or by the relaxation effect. To determine what the main reason is in our case, we used the method of measuring the Auger parameter, whose change ($\Delta\alpha$) equals double the change in the relaxation energy (ΔR), as shown in [43]:

$$\Delta\alpha = \Delta(E_b(Ag3d_{5/2}) + E_{kin}(AgMNN)) = 2\Delta R.$$

The measured values of binding energy and the Auger parameter were described in the form of the dependence graphite surface coverage with silver (Fig. 8b). It is seen that a decrease in E_b with an increase in the size of particles is accompanied by an increase in α ; so the photoelectron shift is at least partly determined by the relaxation effect. The calculation of the contribution of relaxation,

$$\Delta R = 1/2\Delta\alpha = 1/2(0.4) = 0.2,$$

shows that a significant portion (0.3 eV) in the overall shift of the photoelectron line (0.5 eV) is determined by

the effects of the initial state: the well-known metal–nonmetal transition. Note, however, that in contrast to the Auger parameter, which reaches the value characteristic of bulk silver when the size of silver particles reaches 3–5 nm, the binding energy of the $Ag3d$ spectrum remains 0.2 eV higher than E_b for bulk metal (368.2 eV). Only reaching a size of 30–40 nm leads to a further decrease in the binding energy to a value corresponding to the bulk samples. The constant value of the Auger parameter in this range suggests that differential recharging is responsible for this phenomenon [44, 45]. Indeed, if conduction properties of silver start

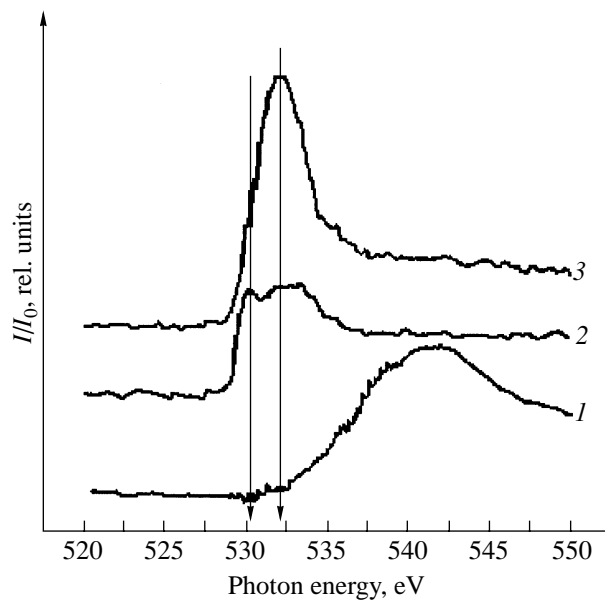


Fig. 5. XANES O K-edge spectrum of (1) electrophilic oxygen and the peroxide state of molecular oxygen adsorbed on the $Ag(110)$ surface [38] measured at (2) sliding and (3) close to normal incident angles of X rays.

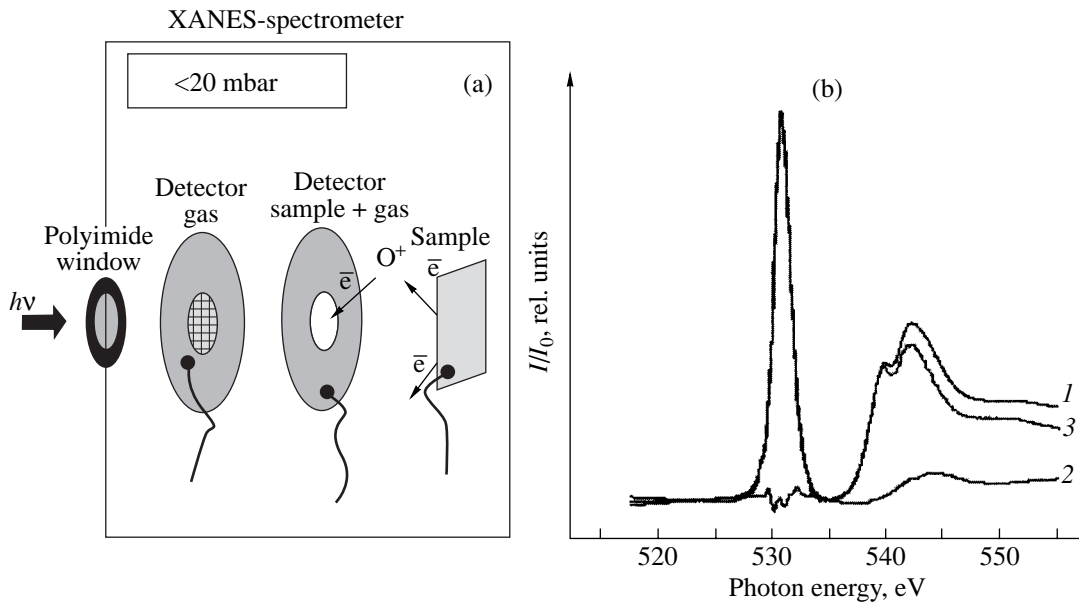


Fig. 6. (a) Schematic of the measuring chamber of the XANES spectrometer separated from the high-vacuum part of the source of synchrotron irradiation by a polyimide window; (b) (1) XANES O K-edge spectra (1) recorded in the course of the interaction of silver foil with the reaction mixture $5\% C_2H_4 + O_2$ at $T = 470$ K and $P = 2 \times 10^2$ Pa, (2) spectrum of the sample surface, and (3) the difference spectrum of the gas-phase spectrum and the complete spectrum.

to reveal themselves at sizes >30 nm, then a positive charge can be accumulated on the surface of silver particles due to photoemission at smaller sizes. This positive charge would increase $E_b(Ag3d_{5/2})$ and decrease $E_{kin}(AgMNN)$ by the same value. As a consequence, the Auger parameter would remain unchanged.

Thus, in the study of electron properties of supported silver particles, we can distinguish two ranges of sizes in which changes in these properties occur before they reach the level of bulk metal. In the first range (3–5 nm), the properties of localized electrons at 4d- and lower levels are formed. In the range of greater sizes (30–40 nm), the properties of conducting electrons are formed. In the case of silver, these are delocalized Ag5s electrons.

Unfortunately, the electron spectrometers used in this study did not allow us to study the surface structure. Therefore, such a study of supported silver clusters was carried out by adsorption of a probe molecule. We used oxygen as a probe molecule. This choice was based on the results presented in [46–48], where it was shown that the efficiency of dissociation of chemisorbed molecular oxygen depends on the structure of the silver surface. In the case of a close-packed Ag(111) plane, heating does not result in the dissociation of molecular oxygen chemisorbed at $T = 120$ K, which almost completely desorbs in the form of O_2 molecules at $T = 220$ K [48]. In contrast to this, the desorption of molecular oxygen chemisorbed on the more open plane (110) with a temperature maximum of 180 K is accompanied by molecular oxygen dissociation [46, 47]. It was assumed that this temperature characterizes the

dissociation of molecular oxygen into atoms rather than desorption. Some of the oxygen desorption is due to the necessity of freeing sites for the dissociation of adsorbed O_2 molecules. To explain the differences in the behavior of molecular oxygen on different planes of silver, Campbell and Paffett [47, 48] assumed that the strength of interaction of the oxygen molecule with the silver surface and, as a consequence, the probability of its dissociation increases with an increase in the degree of surface imperfection. This conclusion allows us to conjecture that the more defects are present on the silver surface, the lower the temperature of dissociation of the molecular form of oxygen adsorption. Therefore, we can expect that chemisorbed atomic oxygen will appear on the defect areas of the surface of silver clusters even at low temperatures of adsorption (e.g., in the range 120–140 K), whereas the presence of the molecular form will indicate that the surface is regular. The applicability of XPS to distinguishing atomic and molecular states of chemisorbed oxygen is determined by a substantial difference in the values of binding energies at which the corresponding O1s spectra are centered: the range 532.2–532.5 eV [15, 35] is characteristic of the molecular form, whereas atomic oxygen is characterized by $E_b \leq 530.5$ eV.

The corresponding O1s spectra recorded for five different coverages of deposited silver after their exposure to molecular oxygen (20000 L) at $T = 130$ K are shown in Fig. 9. It can be seen that the spectra of low coverages are characterized by one, rather narrow line with $E_b = 530.5$ eV, whereas the surface with the maximum surface coverage studied is characterized by the appear-

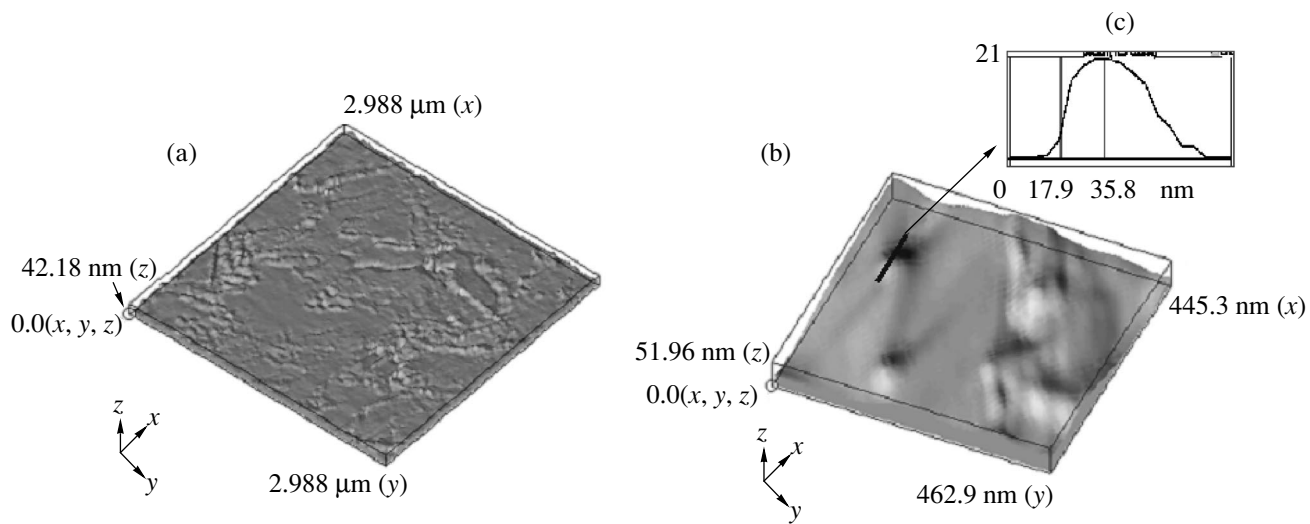


Fig. 7. STM images of the surface of amorphous graphite measured (a) before and (b) after silver deposition (expressed as $I_{\text{Ag}3d}/I_{\text{C}1s} = 13.1$); (b) the profile of heights measured for one of the chosen silver particles.

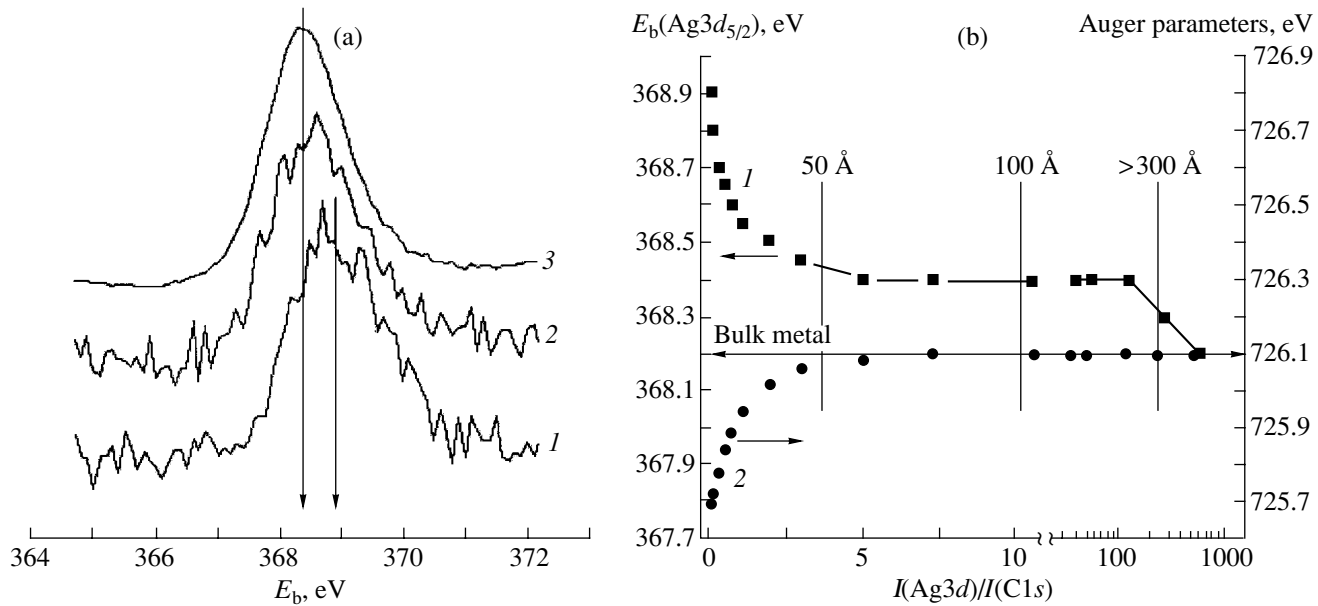


Fig. 8. (a) The $\text{Ag}3d_{5/2}$ spectra of silver deposited on graphite depending on the surface coverage: (1) $\Theta_{\text{Ag}} = 5 \times 10^{13}$, (2) 5×10^{14} , and (3) 5×10^{15} atom/cm²; (b) a plot of the dependence of (1) $E_b(\text{Ag}3d_{5/2})$ and (2) the Auger parameter of silver deposited on graphite on coverage expressed in terms of $I(\text{Ag}3d)/I(\text{C}1s)$.

ance of an additional state with $E_b = 532.2$ eV. The assignment of these signals was based on an analysis of changes in their intensities in the course of sample heating. We found that the disappearance of the band with $E_b = 532.2$ eV occurs when the temperature reaches 220 K. The intensity of the O1s signal at 530.5 eV remains virtually constant up to $T = 470$ K, and this stability is characteristic of all silver coverages studied by us. In agreement with the literature data, such a behavior makes it possible to assign the signals to atomic

($E_b = 530.5$ eV) and molecular (532.2 eV) chemisorbed oxygen. Note that the ratio $\text{O}_{\text{ads}}/\text{O}_{2,\text{ads}}$ depends on the graphite coverage with silver. Because silver was deposited at room temperature and the sample was cooled only then, it is correct to consider not the coverage but the size of the silver particles. STM data for several coverages (Figs. 7, 8) were used to translate silver coverages into the sizes of silver particles. We found that the appearance of molecular adsorbed oxygen occurs on the surface of particles with an average

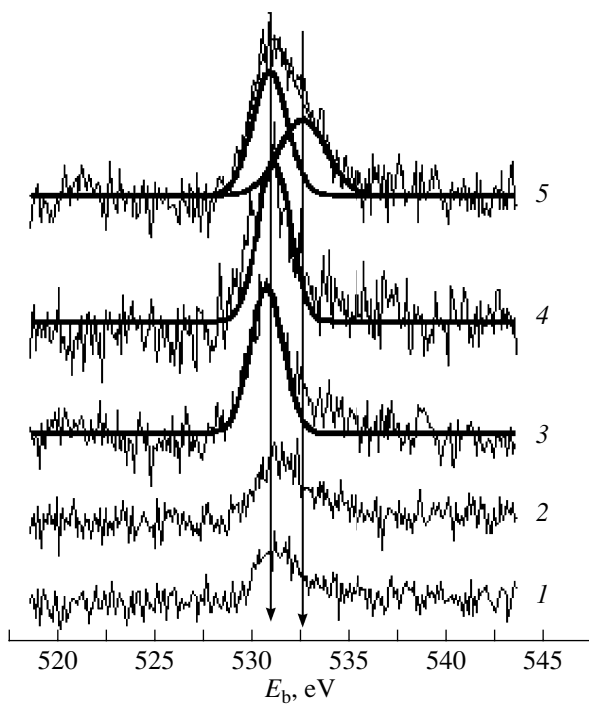


Fig. 9. XPS spectra of O1s recorded after adsorption of O₂ at $T = 130$ K (the exposure is 20000 L) on the silver surface deposited on graphite depending on the coverage $I_{\text{Ag}3d}/I_{\text{C}1s}$: (1) 1.0, (2) 2.0, (3) 9.5, (4) 23, and (5) 550.

size of ~ 50 nm. The absence of molecular states for low coverages allows one to suggest that the surface of small particles (up to 30 nm) is shown by defect low-coordinated atoms, and this provides a high degree of O₂ molecule dissociation at a temperature as low as 130 K. The appearance of chemisorbed molecular oxygen for large silver particles (≥ 50 nm) points to the formation of smooth areas with a (111)-like structure. Note that this range of sizes coincides with the range of changes in the properties of conduction electrons. It is likely that these two effects are related.

The deviation of electron and structural properties of silver particles on the properties of bulk metal with a decrease in their sizes assumes that the reactivity of supported metallic particles toward gas-phase molecules should also change depending on their size. Figure 10a shows the O1s spectra recorded after O₂ adsorption for 30 min at $P = 10$ Pa and $T = 420$ K. We note once again that, in the case of bulk silver, these conditions led to the formation of only nucleophilic O_{ads}. In contrast to this, on the surface of small silver particles electrophilic oxygen is formed, as suggested by the appearance of the O1s line in the spectrum with $E_b \sim 530.5$ eV. Electrophilic oxygen dominates up to 30-nm silver particles. A further increase in the size of silver particles leads to the appearance of the O1s band, which is characteristic of nucleophilic oxygen.

Thus, the same two forms of adsorbed oxygen as in the case of bulk silver samples, nucleophilic and elec-

trophilic, are registered on the surface of supported silver particles, but there is a substantial difference: for the formation of O_{elec}, the simple adsorption of pure O₂ rather than its mixture with ethylene is enough. This allows us to hope that the registration of its TPR spectrum and, accordingly, the determination of the strength of its binding to the silver surface is possible, unlike in the case of bulk silver when dissolved oxygen desorption has a masking effect and when it is eliminated via a possible reaction with near-surface carbon formed in the course of silver surface activation with the reaction medium.

To carry out TPD experiments, a graphite layer was prepared on the surface of tantalum foil that was heated by resistance with a ramp of 2–3 K/s by ethylene decomposition at $T = 1100$ K and $P = 5 \times 10^3$ Pa [40]. The time of decomposition was controlled by recording the overview spectrum until the complete disappearance of tantalum signals. The conclusion about the graphite nature of the supported carbon layer was drawn on the basis of the coincidence of its spectral characteristics (position of the C1s band and the existence of the shake-up satellite) with the corresponding characteristics of bulk graphite [16]. The preparation of a graphite layer was carried out in the chamber of electron spectrometer where further vacuum deposition and oxygen adsorption were carried out.

Figure 10b shows the TPD spectra of electrophilic oxygen recorded using both mass spectrometry according to O₂ desorption to the gas phase (curve 1) and a change in the intensity of the O1s signal with $E_b = 530.5$ eV (curve 2) after its differentiation (the procedure for obtaining the TPD spectra using XPS data was described in [49]). The complete coincidence of these spectra proves that it is the desorption of electrophilic oxygen that is responsible for the appearance of these spectra. The lower temperature of electrophilic oxygen desorption (500 K) compared to nucleophilic oxygen O_{ads} desorption (580 K) suggests that oxygen participating in ethylene epoxidation binds less strongly with the silver surface than oxygen active in the complete oxidation of C₂H₄ to CO₂ and H₂O. This result is very important, because it means that the thermodynamic condition for the participation of this oxygen form in the formation of ethylene oxide is fulfilled [30, 50]: the estimated upper limit of the bond strength of oxygen responsible for ethylene epoxidation is 25–27 kcal/mol.

Another specific feature of supported silver is a change in the relative population of these O_{ads} species depending on the size of particles. The nature of this behavior makes it possible to explain the size effect in ethylene epoxidation in the framework of a unified reaction mechanism, when the rate of this reaction on the Ag/α-Al₂O₃ catalysts decreases by more than an order of magnitude with a decrease in the average size of silver particles below 50 nm [51]. The absence of nucleophilic adsorbed oxygen on small silver particles leads to a decrease in the concentration of adsorbed eth-

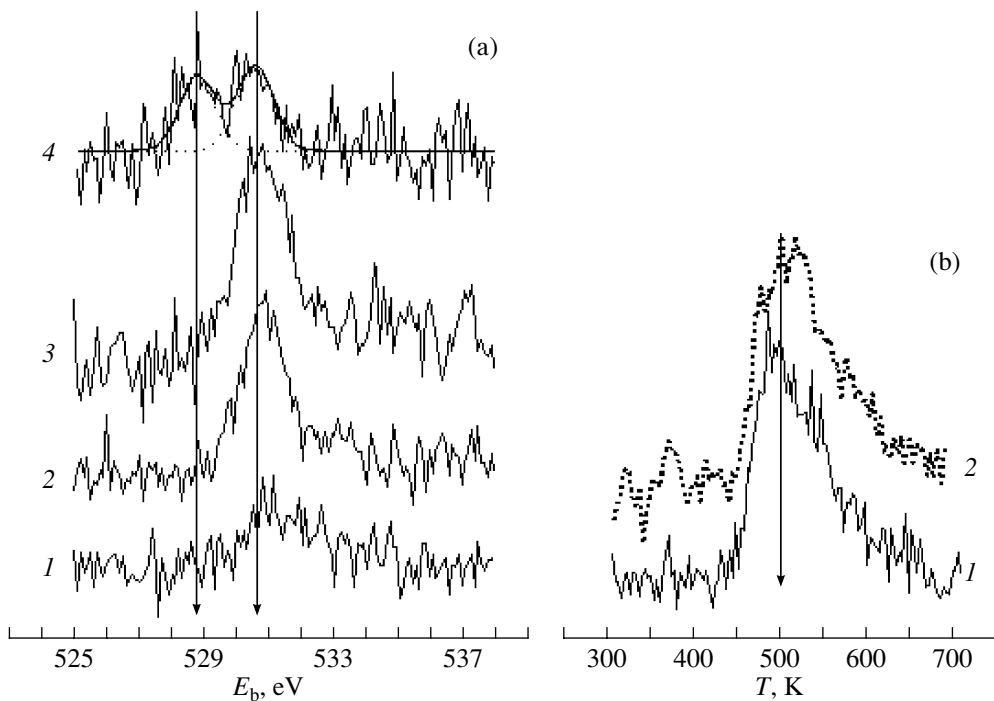
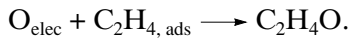
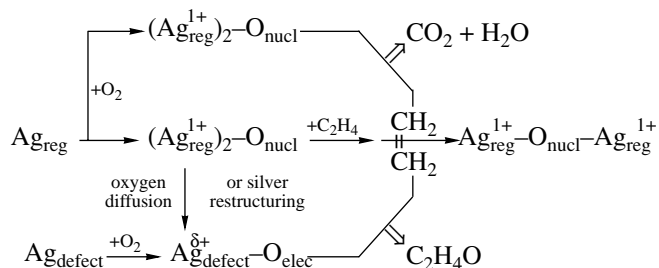


Fig. 10. (a) XPS spectra O1s recorded after adsorption of O₂ for 10 min at $T = 420$ K and $P_{O_2} = 10$ Pa on the surface of silver deposited on graphite depending on the surface coverage I_{Ag3d}/I_{C1s} : (1) 0.4, (2) 1.5, (3) 2.4, and (4) 13.1; (b) TPD spectra of O₂ measured by (1) mass spectrometry and (2) using a change in O1s intensity for the coverage $I_{Ag3d}/I_{C1s} = 2.4$.

ylene, which according to the surface action law leads to a decrease in the rate of the key epoxidation reaction:



This can serve as an additional argument in favor of the fact that both electrophilic and nucleophilic oxygen adsorbed on silver are involved in the composition of the active site of ethylene epoxidation.



Oxygen adsorption on the regular silver surface (Ag_{reg}) leads to the formation of nucleophilic adsorbed oxygen, which creates sites for ethylene adsorption and is only active in the reaction of complete oxidation. Only the transformation of regular areas of the surface into the defect surface (Ag_{defect}) due to silver activation by the components of the reaction medium leads to the formation of electrophilic O_{ads} , which forms the key

CONCLUSIONS

As a result of the fundamental study of the nature and reactivity of various forms of adsorbed oxygen when considering the problems of pressure and material gap, we proposed the following mechanism of ethylene epoxidation:

product in the reaction with adsorbed ethylene. The formation of electrophilic oxygen is possible in the direct adsorption of O₂ if it occurs on defective silver, as in the case of supported silver particles with sizes <50 nm. The surface of these particles consists of low-coordinated atoms with a deficient electron density.

Understanding the molecular mechanism of the reaction should lead researchers to predict the catalytic

properties of catalyst samples and to suggest better ways for improving catalytic systems. Because one of the main characteristics of commercial ethylene epoxidation is the yield of the target product, ethylene oxide, one should first analyze factors affecting the process selectivity. The selectivity to ethylene oxide,

$$S = \frac{w(C_2H_4O)}{w(C_2H_4O) + w(CO_2)},$$

is determined by the ratio of the rates of epoxidation and complete oxidation.

In the case of bulk silver, the efficient formation of nucleophilic oxygen compared to the low rate of electrophilic oxygen formation (due to surface modification by the components of the reaction mixture) leads to the high rate of the complete oxidation pathway. Therefore, despite rather high epoxidation reaction rates, the selectivity of silver single crystals is rarely higher than 30–40% [5, 6, 29]. In the case of supported catalysts, the rate of epoxidation is two orders of magnitude lower because of a decrease in the concentration of sites (Ag^{1+}) for ethylene chemisorption. The rate of direct complete oxidation by ionic oxygen decreases simultaneously but more drastically than the epoxidation rate because of the difference in the stoichiometry of interaction with oxygen: C_2H_4 oxidation to CO_2 and H_2O requires six oxygen atoms instead of one. This leads to an increase in the selectivity of reaction in the case of supported samples. Indeed, papers devoted to supported catalysts rarely report values of selectivity lower than 50% [52]. If the reaction mechanism described above is correct, than a decrease in the average size of silver particles, especially in the range below 50 nm, should lead to a further increase in the selectivity (even above 86%), which is a limiting value in the case of the molecular form of oxygen responsible for ethylene epoxidation: $S < 6/7$ [5, 6]. In contrast to this, several researchers reported data on a decrease in the selectivity with a decrease in the size of silver particles [53], which can be explained without considering the contribution of secondary reactions of further oxidation of ethylene oxide on the alumina surface. Indeed, if the formation of ethylene oxide only occurs on the silver surface (see above), the formation of complete oxidation products is possible at least via two pathways (complete oxidation of ethylene by nucleophilic oxygen adsorbed on silver and the reaction of ethylene oxide oxidation to CO_2 and H_2O), to which the reaction on the support (Al_2O_3) surface contributes most greatly. If this assumption is correct, then the high selectivity is achieved if ethylene oxide oxidation is suppressed. As shown in one of the mechanistic studies of these reactions [54], they are catalyzed by acidic OH groups on the alumina surface. Therefore, it is clear that one of the methods for solving this problem may be the use of a support without such sites on the surface. Indeed, the replacement of alumina by a carbon support (sibunit) made it possible to reach a selectivity of 85–88%. In the

case of ultradispersed silver powder, when silver particles with average sizes were close to optimal (50–100 nm) in the absence of any support, the selectivity was even higher (>90%) [55]. These results prove the correctness of the proposed mechanism and the methodology described in this review, which is based on a surface science study of adsorbed species in connection with the study of reasons behind the catalytic action of heterogeneous systems.

ACKNOWLEDGMENTS

I thank B.S. Balzhinimaev, A.I. Boronin, V.V. Kachev, R.I. Kvon, I.P. Prosvirin, A.F. Carley, M.W. Roberts, A. Knop-Gericke, M. Hävecker, and R. Schlögl for their help in carrying out experiments and fruitful discussions of the results of this work. This work was supported by the Russian Foundation for Basic Research (grant nos. 96-03-33891 and 00-15-99335) and the Fund for the Support of National Science (support of young doctors of science).

REFERENCES

1. Goodman, D.W., *Surf. Sci.*, 1994, vols. 299/300, p. 837.
2. Bukhtiyarov, V.I., *Interfacial Science*, Roberts, M.W., Ed., Oxford: Blackwell Sci., 1997, p. 109.
3. Freund, H.-J., Kuhlenbeck, H., Libuda, J., Rupprechter, G., Bäumer, M., and Hamann, H., *Top. Catal.*, 2001, vol. 15, p. 201.
4. Besenbacher, F., Chorkendorff, I., Clausen, D.S., Hammer, B., Molenbroek, A.M., Norskov, J.K., and Stensgaard, I., *Science*, 1998, vol. 279, p. 1913.
5. Campbell, C.T. and Paffett, M.T., *Surf. Sci.*, 1984, vol. 139, p. 396.
6. Campbell, C.T. and Paffett, M.T., *J. Catal.*, 1985, vol. 94, p. 436.
7. Joyner, R.W. and Roberts, M.W., *Chem. Phys. Lett.*, 1979, vol. 60, p. 459.
8. Bukhtiyarov, V.I. and Prosvirin, I.P., *Proc. Eur. Congr. on Catalysis* (Europacat VI), Limerick, Ireland, 2001, p. 21.
9. Hävecker, M., Knop-Gericke, A., Sheld-Niedrig, Th., and Schlögl, R., *Top. Catal.*, 2001, vol. 15, p. 27.
10. Ozensoy, E., Meier, D.C., and Goodman, D.W., *J. Phys. Chem.*, 2002, vol. 106, p. 9367.
11. Rupprechter, G., Unterhalt, H., Morkel, M., Galletto, P., Hu, L., and Freund, H.-J., *Surf. Sci.*, 2002, vols. 502–503, p. 109.
12. Kachev, V.V., Unterhalt, H., Prosvirin, I.P., Bukhtiyarov, V.I., Rupprechter, G., and Freund, H.-J., submitted to *J. Phys. Chem.*
13. Xu, X., Szanyi, J., Xu, Q., and Goodman, D.W., *Catal. Today*, 1994, vol. 21, p. 57.
14. Baumer, M. and Freund, H.-J., *Prog. Surf. Sci.*, 1999, vol. 61, p. 12.
15. Rao, C.N.R., Vijayakrishnan, V., Santra, A.K., and Prins, M.W.J., *Angew. Chem., Int. Ed. Engl.*, 1992, vol. 31, p. 1062.

16. Bukhtiyarov, V.I., Carley, A.F., Dollard, L.A., and Roberts, M.W., *Surf. Sci.*, 1997, vol. 381, p. 605.
17. Unterhalt, H., Rupprechter, G., and Freund, H.-J., *J. Phys. Chem. B*, 2002, vol. 106, p. 356.
18. Rumpf, F., Popa, H., and Boudart, M., *Langmuir*, 1988, vol. 4, p. 722.
19. Engel, T. and Ertl, G., *J. Chem. Phys.*, 1978, vol. 69, p. 1267.
20. Engel, T. and Ertl, G., *Adv. Catal.*, 1979, vol. 22, p. 2.
21. Stara, I. and Matolin, V., *Surf. Sci.*, 1994, vol. 313, p. 99.
22. Doering, D.L., Popa, H., and Dickinson, J.T., *J. Vac. Sci. Technol.*, 1982, vol. 20, p. 827.
23. Altman, E.I. and Gorte, R.J., *Surf. Sci.*, 1988, vol. 195, p. 392.
24. Herskowitz, M., Holliday, R., Cutlip, M.B., and Kennedy, C.N., *J. Catal.*, 1982, vol. 74, p. 408.
25. Altman, E.I. and Gorte, R.J., *Surf. Sci.*, 1986, vol. 172, p. 71.
26. Oh, S.H. and Eickel, C.C., *J. Catal.*, 1991, vol. 128, p. 526.
27. Xu, X. and Goodman, D.W., *Catal. Lett.*, 1994, vol. 24, p. 31.
28. Kuhn, W.K., Szanyi, J., and Goodman, D.W., *Surf. Sci.*, 1992, vol. 274, p. L611.
29. Grant, R.B. and Lambert, R.M., *J. Catal.*, 1985, vol. 92, p. 364.
30. Van Santen, R.A. and de Groot, C.P.M., *J. Catal.*, 1986, vol. 98, p. 530.
31. Bukhtiyarov, V.I., Boronin, A.I., Prosvirin, I.P., and Savchenko, V.I., *J. Catal.*, 1994, vol. 150, p. 262.
32. Boronin, A.I., Avdeev, V.I., Koshcheev, S.V., Murzakhametov, K.T., Ruzankin, S.F., and Zhidomirov, G.M., *Kinet. Katal.*, 1999, vol. 40, no. 5, p. 721.
33. Rovida, G., Pratesi, F., Maglietta, M., and Ferroni, F., *Surf. Sci.*, 1974, vol. 43, p. 230.
34. Barreau, M.A. and Madix, R.J., *Surf. Sci.*, 1984, vol. 140, p. 108.
35. Carley, A.F., Davies, P.R., Roberts, M.W., and Thomas, K.K., *Surf. Sci.*, 1990, vol. 238, p. L467.
36. Barreau, M.A. and Madix, R.J., *J. Electron Spectrosc. Relat. Phenom.*, 1983, vol. 31, p. 101.
37. Stöhr, J., *NEXAFS Spectroscopy*, Berlin: Springer, Gomer R., Ed., 1992, vol. 25.
38. Pawela-Crew, J., Madix, R.J., and Stohr, J., *Surf. Sci.*, 1995, vol. 339, p. 23.
39. Kaichev, V.V., Bukhtiyarov, V.I., Khavker, M., Knop-Gerike, A., Maier, R.V., and Shlegel, R., *Kinet. Katal.*, 2003, vol. 44, no. 3, p. 471.
40. Bukhtiyarov, V.I. and Kaichev, V.V., *J. Mol. Catal. A: Chem.*, 2000, vol. 158, p. 167.
41. Mason, M.G., *Phys. Rev. B*, 1983, vol. 27, p. 748.
42. Wertheim, G.K. and Di Cenzo, S.B., *Phys. Rev. B*, 1988, vol. 37, p. 844.
43. Wagner, C.D., *Faraday Disc.*, 1975, no. 60, p. 291.
44. Barr, T.L., *J. Vac. Sci. Technol.*, A, 1989, vol. 7, p. 1677.
45. Bukhtiyarov, V.I., Prosvirin, I.P., and Kvon, R.I., *J. Electron Spectrosc. Relat. Phenom.*, 1996, vol. 77, p. 7.
46. Backx, C., de Groot, C.P.M., Biloen, R., and Sachtler, W.M.H., *Surf. Sci.*, 1981, vol. 104, p. 300.
47. Campbell, C.T. and Paffett, M.T., *Surf. Sci.*, 1984, vol. 143, p. 517.
48. Campbell, C.T., *Surf. Sci.*, 1985, vol. 157, p. 43.
49. Bukhtiyarov, V.I., Kaichev, V.V., Podgornov, E.A., and Prosvirin, I.P., *Catal. Lett.*, 1999, vol. 57, p. 233.
50. Khasin, A.V., *Kinet. Katal.*, 1993, vol. 34, no. 1, p. 42.
51. Bukhtiyarov, V.I., Prosvirin, I.P., Kvon, R.I., Goncharov, S.N., and Bal'zhinimaev, B.S., *J. Chem. Soc., Faraday Trans.*, 1997, vol. 93, p. 2323.
52. Sajkowski, D.J. and Boudart, M., *Catal. Rev.-Sci. Eng.*, 1987, vol. 29, p. 325.
53. Goncharova, S.N., Paukshtis, E.A., and Bal'zhinimaev, B.S., *Appl. Catal. A*, 1995, vol. 126, p. 67.
54. Bulushev, D.A., Paukshtis, E.A., Nogin, Yu.N., and Bal'zhinimaev, B.S., *Appl. Catal.*, 1995, vol. 123, p. 301.
55. Bal'zhinimaev, B.S., Zaikovskii, V.I., Pinaeva, L.G., Romanenko, A.V., and Ivanov, G.V., *Kinet. Katal.*, 1998, vol. 39, p. 714.